

THE SYNTHETIC GEOID AND THE ESTIMATION OF MESOSCALE ABSOLUTE TOPOGRAPHY FROM ALTIMETER DATA

A “synthetic geoid” is an estimation of the medium spatial scale variations of the true marine geoid. It is calculated by subtracting from an altimeter-derived mean sea surface an estimate of mean sea-surface displacement obtained from a dynamical ocean model initialized with remotely sensed and *in situ* data. Estimates of the absolute sea-surface topography for oceanic mesoscale variability (current meanders and eddies) are obtained from Geosat altimetric data using a synthetic geoid and are compared with observations and model results. This method is compared with results obtained by differencing sea-surface heights along individual tracks from the altimetric mean sea surface and with those obtained by differencing two individual repeat tracks from each other. Excellent results are obtained for the Gulf Stream region, for several cases of the ocean region between Greenland and the United Kingdom, and for an isolated eddy observed in the northeastern Atlantic Ocean.

INTRODUCTION

The fundamental measurement made by a satellite-borne radar altimeter is the distance from the active sensor to the surface of the sea on the Earth below. The signal important to the oceanographer pursuing dynamical research, “nowcast” schemes, and forecast models is the departure of the sea surface away from the geoid as a function of position and time. The displacement is called the sea-surface height or absolute dynamical topography. The geoid, which is not known with sufficient precision for ocean dynamics studies, is the gravitational equipotential surface to which the sea surface would relax if all internal motions in the ocean were to cease. Because of gravity anomalies and other irregularities, the geoid differs significantly from the ellipsoidal surface corresponding to a uniformly rotating homogeneous planet. Differences from such a reference surface occur on many scales and have amplitudes on the order of several tens of meters.

The oceanographic signal itself is variable on a wide range of time and space scales because of the variety of dynamical phenomena occurring in the sea. High-frequency phenomena, such as tides, are regarded as environmental noise to be removed from the signal of interest. The most energetic phenomenon in the ocean is the so-called mesoscale variability, which arises from the meandering of currents and jets and the motions of related rings and eddies or fields of mid-ocean eddies. These meanders and eddies are the “internal weather” of the ocean. Vertically they extend smoothly throughout the water column, and their surface-pressure field and its associated sea-surface height reflect the deeper flow. Height signals are typically on the order of a few tens of centimeters, but many of the strongest currents reach a meter. Time scales span a few days to a few months, and space scales are on the order of several tens of kilo-

meters to a few hundred kilometers. The general circulation of the ocean has a basin-scale component (about 1000 km) that is interesting and important, but the associated sea-surface heights are measured in tens of centimeters over thousands of kilometers.

The mean circulation of the ocean, however, also has sub-basin-scale structures caused by the existence and variability of major current and frontal systems, such as the mean dynamic topography resulting from a meandering current system. The mean sea-surface-height signal will retain the strength of the instantaneous current, but will be smeared across the envelope of the meandering (e.g., the Gulf Stream has an instantaneous width of 80 km but a mean envelope 100–300 km across). The ocean circulation is heterogeneous, and the eddy kinetic energy (EKE) is usually larger than the mean kinetic energy (MKE), but the former can be comparable to or occasionally less than the latter. The frequency of occurrence and the structure of meanders and eddies determine the relative contribution of the rectified mesoscale variability to the mean sea-surface height, compared with the contribution of the steady, large-scale flow to the mean sea-surface height.

We focus in this article on the mesoscale absolute dynamic topography, that is, the variations in sea-surface height induced by the dynamics of the ocean’s mesoscale currents and features. The amplitude of the dynamical ocean-surface displacement, measured as a departure from a reference ellipsoid along any specific altimetric track, is on the order of a meter or less (one or two orders of magnitude smaller than the displacement resulting from geoid variations). In addition to the geoid and the dynamic topography, the return-radar pulse to the altimeter is influenced by atmospheric and surface effects. It also contains noise from instrumental, system,

and orbit errors, which are treated by well-established methods.¹ The orbit error of interest here is a relatively long wavelength, several thousands of kilometers, with an amplitude of a few meters, and can be modeled by simple analytic functions (such as bias, linear, and quadratic). We typically analyze a track of a few thousand kilometers, even if the region being studied is smaller. Orbit error is nearly eliminated by removing all the energy from the measurement that can be fit with a quadratic function, leaving no tilt or bias in the remaining signal. This operation also removes the smaller-amplitude, large-scale component of the dynamic topography, but with negligible effect on the shorter, relatively energetic mesoscale features.

Consider now for a satellite-borne altimeter in an exactly repeating orbit the extraction of the oceanographic signal from the fundamental measurement by some means of estimating or eliminating the geoid. (Geosat repeats its tracks every 17.05 days.) Averaging over a set of measurements along one track yields the altimetric mean sea surface composed of the geoid and the mean dynamical topography (mean oceanography) on scales left after the large-scale error and signal are removed by the quadratic model. The mean oceanography remaining is in the form of sub-basin-scale structures caused, for example, by mesoscale motions including meandering or rectification. If some method of independently estimating and subtracting the mean oceanography were available, the remainder would yield a geoid estimate suitable for use in the extraction of the mesoscale oceanographic signal from the analyzed altimeter data. We call this geoid estimate a synthetic geoid because it is not an absolute estimate and contains only a limited range of scales of geoidal structure.

We will discuss three methods for comparison. The first method, pass minus synthetic geoid, entails differencing individual tracks from a synthetic geoid. It produces absolute mesoscale signal estimates that are directly interpretable. Little is known about the oceans, however, and the required mean oceanography estimate is often not available. The second method, pass minus mean sea surface, involves differencing the individual tracks from the altimeter-derived mean sea surface. In regions where no sub-basin-scale mean features exist (i.e., the long-term mean approaches zero), the estimate of the mean sea surface is the synthetic geoid, making this method equivalent to the first. But where sub-basin mean oceanography exists, for example in the Gulf Stream and the Greenland, Iceland, United Kingdom (GIUK) Gap, the method can make an already small oceanographic signal even weaker. Thus, experience, conceptual models, and ancillary data are necessary to interpret the features of the instantaneous mesoscale from the resultant signal. The third method, pass minus pass, does not involve the altimetric mean; rather, two individual repeat tracks are differenced, which removes both the time-independent ocean signal and the geoid and yields the difference signal of the instantaneous mesoscale features at the two times. If the mesoscale features are simple and well separated spatially, interpretation is easy; if the features overlap, however, partial

cancellation and complex signals can occur that require experience or independent *a priori* estimates for interpretation. An advantage of the pass-minus-pass method is the rapidity with which one can initiate work in a new region.

The Harvard open-ocean model^{2,3} has for the past several years been used as a component of nowcast and forecast schemes in various regions of the world's oceans. It uses data for its initialization and assimilates data during its operation. In particular, time series of mesoscale resolution maps of sea-surface height have been generated for the Gulf Stream meander and ring region and the region of the East Iceland Polar Front between Iceland and the Faeroe Islands. Such time series provide the data required to generate the mean oceanography input to synthetic geoid estimates. We are conducting research with synthetic geoids in both regions. The Gulf Stream region has a strong sea-surface-height signal (of the order of 1 m), and there the pass-minus-synthetic geoid method is proving successful and powerful. The signal in the East Iceland Polar Front (of the order of 20 cm) presents a more difficult problem, but preliminary results are encouraging.

This article, which is a preliminary report of work in progress, focuses on the synthetic geoid methodology, its applicability in various regimes of oceanic mesoscale variability, its validation, and its comparison with other methods. We present the theory and discuss the Gulf Stream—where the mesoscale signal is strong—in terms of the mean oceanography, the synthetic geoid, and comparisons with sea-surface height estimates based on the model and on *in situ* data. We compare the three methods using a real-time example and also present first results for the East Iceland Polar Front (the GIUK Gap) and the northern northeast Atlantic. The latter region has occasional strong eddies in a weak background flow, so that the synthetic geoid requires no mean oceanography.

DERIVATION OF RELEVANT EQUATIONS

The altimeter on board Geosat measures the instantaneous height of the satellite above the sea surface ten times per second, and measurements are averaged over 1 s for a nominal spacing of 6.7 km along the ground track. The computed ephemeris of the satellite is then used along with the altimeter observations to determine the height of the sea surface above the reference ellipsoid. The sea-surface height is corrected for the effects of the tides, electromagnetic bias, troposphere, and ionosphere, after the method of Cheney et al.,¹ and the data are interpolated and edited according to the criteria of Porter et al.⁴

The 1-s-average estimates of sea-surface height obtained during pass *i* may be written as

$$H_i = G + O_i + E_i + \epsilon_i, \quad (1)$$

where *G* is the elevation of the true geoid above the reference ellipsoid, *O_i* is the sea-surface height due to the ocean dynamics, *E_i* is the height due to the unknown orbit error (i.e., the difference between where the satel-

lite actually is and where the computed ephemeris says it is), ϵ_i is the error in the altimeter measurement, and the subscript i is the index of the pass. Typically, G is of the order of 10 m, E is of the order of 1 m, O is 1 m or less, and ϵ is of the order of 0.05 m.

The geoid G does not change as a function of time. The oceanic term O_i is the height variation of the sea surface caused by currents and eddies on all scales. The orbit error E_i may be decomposed into two parts. The first is the long-wavelength error of the order of 40,000 km produced by errors in the initial conditions used to compute the ephemeris. The second part results from errors in the gravity model used to compute the orbit. The satellite integrates the errors in the gravity model as it travels over the ground track. If the same orbit is repeated, the satellite will integrate the same errors, so that the only difference in orbit error between the two passes will result from the errors in the initial conditions.⁵

Data gaps in the altimetric measurements along the Geosat ground track occur when the satellite tilts away from nadir, causing the altimeter to lose signal acquisition of the sea surface. To deal technically with such data dropouts, we select a reference pass free of dropouts (or, alternatively, the pass with the fewest dropouts), where $i = R$ in Equation 1. The orbit error associated with pass i can be written in terms of the orbit error of the reference pass:

$$E_i = E_R + E_i' . \quad (2)$$

The sea-surface height of pass i is now subtracted from the sea-surface height of the reference pass for each point along the track, and a quadratic equation is fitted to the along-track difference using the method of least squares. The least-squares fit of the quadratic equation is a high-pass filter that removes the long-wavelength terms such as the dominant orbit error but passes the shorter-wavelength mesoscale features. The quadratic function Q_i is fit in the least-squares method to the large-scale oceanography and the large-scale orbit error, and is written symbolically as

$$Q_i = - E_i' + (O_R - O_i)_L , \quad (3)$$

where the subscript L means the dynamically forced sea-surface height that can be fit by a quadratic equation over the arc used to compute the mean (e.g., the 2500-km-long Gulf Stream arc). Now Q_i can be added to Equation 1 to obtain a sea-surface height \tilde{H}_i that has the long-wavelength component relative to the reference pass removed:

$$\begin{aligned} \tilde{H}_i &= G + O_i - (O_i)_L + (O_R)_L \\ &+ E_R + \epsilon_i . \end{aligned} \quad (4)$$

The altimetric mean sea surface can now be formed by averaging over all the cycles, so that

$$\begin{aligned} \langle \tilde{H} \rangle &= G + \langle O \rangle - \langle O_L \rangle + (O_R)_L \\ &+ E_R + \langle \epsilon \rangle . \end{aligned} \quad (5)$$

Except for the geoid and the orbit error caused by the reference pass, the dominant term in Equation 5 is $\langle O \rangle$. The other terms are small. The synthetic geoid S_G can be computed from $\langle O \rangle$ by subtracting the mean oceanography $\langle O_{HM} \rangle$ as derived from the Harvard model:

$$\begin{aligned} S_G &= G + [(\langle O \rangle - \langle O_{HM} \rangle) \\ &- \langle O_L \rangle + (O_R)_L + E_R + \langle \epsilon \rangle] . \end{aligned} \quad (6)$$

The absolute topography S_i can be computed by subtracting the synthetic geoid S_G from the individual pass \tilde{H}_i :

$$\begin{aligned} S_i &= O_i - [(\langle O \rangle - \langle O_{HM} \rangle) + (O_i)_L \\ &- \langle O_L \rangle - (\epsilon_i - \langle \epsilon \rangle)] . \end{aligned} \quad (7)$$

The dominant term on the right side of the equation is O_i , the dynamical oceanographic signal.

Using these equations, an estimate of the sea-surface height relative to the mean sea-surface height can be written as

$$\begin{aligned} R_i &= (O_i - \langle O \rangle) - [(O_i)_L - \langle O_L \rangle] \\ &+ (\epsilon_i - \langle \epsilon \rangle) . \end{aligned} \quad (8)$$

The pass-minus-pass differences D_{ij} can be written as

$$D_{ij} = (O_i - O_j) - [(O_i)_L - (O_j)_L] + (\epsilon_i - \epsilon_j) . \quad (9)$$

In all the estimates, the geoid and the orbit error due to the reference pass exactly cancel.

We have, then, three powerful tools for interpreting the mesoscale oceanographic signals: (1) the pass-minus-synthetic geoid, (2) the pass-minus-mean sea surface, and (3) the pass-minus-pass differences.

APPLICATION TO THE GULF STREAM

Gulf Stream Model Mean Field

The Harvard open-ocean model^{2,3} is the dynamical component of an operational "Gulfcast" scheme. Daily forecasts of Gulf Stream and eddy positions are projected weekly.⁶ Results have been accumulated over two years. The model uses quasi-geostrophic baroclinic dynamics and can employ a surface-boundary-layer component with higher-order physics.⁷ The strong oceanographic features such as those of the Gulf Stream and its associated eddies can be modeled by analytic functions. The position of these functions in the initialization of the nowcast is determined from ocean observations.⁸ A Gulf Stream and eddy nowcast is used to form the initial conditions of the model, as shown in the contour map of streamlines in Figure 1A. The Gulf Stream axis and eddy locations are determined from satellite infrared imagery, temperature and depth data from aircraft-launched expendable bathythermographs (AXBT),⁹ and, more recently, altimeter data. After the initial condi-

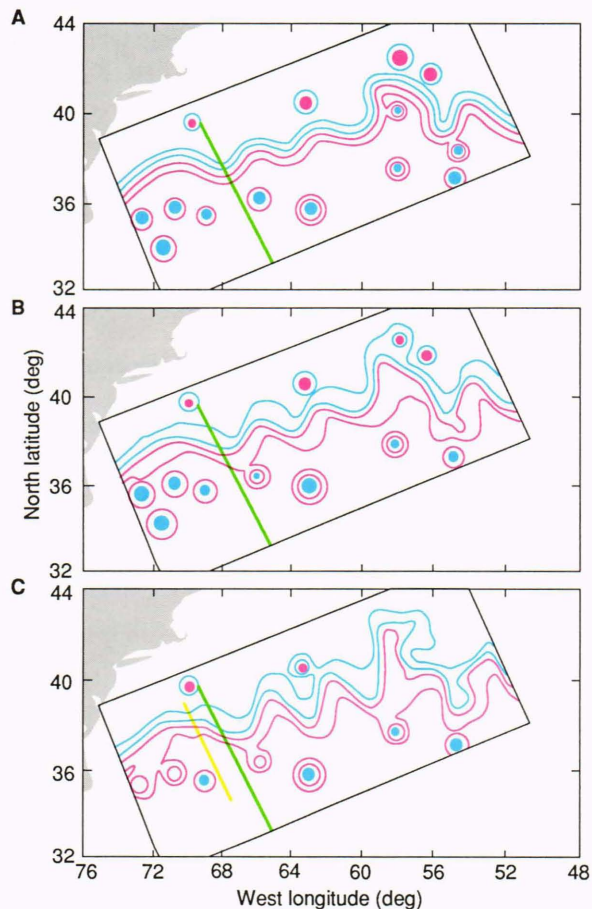


Figure 1. A. The nowcast used for initialization of a Gulf Stream forecast based on satellite infrared imagery and Geosat altimetric data for 12 April 1989. B. Day 3 of the forecast for 15 April 1989. C. Day 7 of the forecast for 19 April 1989. The contours show the streamlines at a 100-m depth; the blue lines represent negative values. A solid blue center indicates a cold ring and a solid red center indicates a warm ring. The Geosat ground tracks are shown in green and yellow.

tions of the model are set, the model generates daily forecasts for 1 week; days 3 and 7 of the forecast are shown in Figures 1B and 1C, respectively. From 19 November 1986 through 11 January 1989, these operational forecasts were generated weekly in real time. The nowcasts and forecasts provide a unique set of estimates of the daily position of the Gulf Stream and its associated rings.

A mean sea surface, shown in Figure 2, was formed by averaging 364 of the daily Gulfcasts from 7 October 1987 to 4 October 1988. Other averaging schemes were also examined (e.g., averaging just the 52 nowcasts), but little difference was found between them. The mean sea surface along each satellite ground track over the model domain was obtained by sampling the averaged model sea surface, an example of which is the Geosat ascending track shown in the figure. Future work will investigate the use of matched averages, that is, only averaging the model results along a specific satellite track when the altimeter is acquiring data.

Geosat Altimetric Mean Field

To compute the altimetric mean sea surface along the sample track shown in Figure 2, a reference pass was selected that terminated at the 2250-m isobath. The reference pass was chosen to be the pass that had the most data over the length of arc, nominally 2500 km. Next, another pass was selected for study (the new pass and the reference pass having different orbit errors). We remove the orbit error by differencing the new pass and the reference pass using the methods described previously. This process eliminates all long-wavelength components from the signal, including the long-wavelength ocean signals. Once the procedure is carried out for all the passes, the 1-year-mean sea surface can be computed.

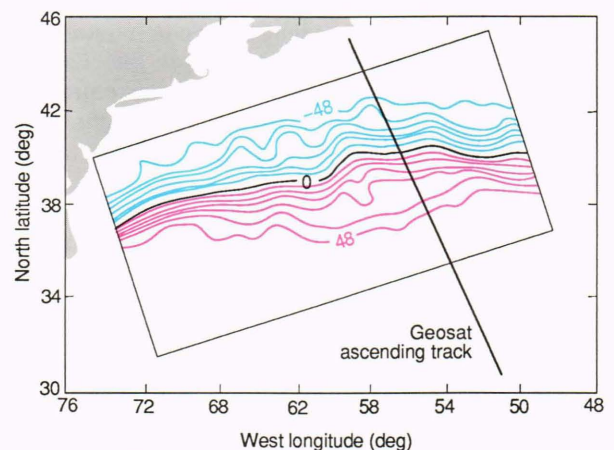


Figure 2. Isopleths of constant sea-surface topography, in intervals of 8 cm, for a 1-year average of the Gulf Stream model. The line perpendicular to the stream is an ascending Geosat track. Refer to Figure 1 caption for color code. (Reproduced, with permission, from Porter, D. L., Glenn, S., and Robinson, A. R., "Geoid Estimates in the Gulf Stream from GEOSAT Altimetry Data and a Gulfcast Mean Sea Surface," in *IGARSS '89, 12th Canadian Symposium on Remote Sensing, Quantitative Remote Sensing: An Economic Tool for the Nineties*, Vol. 2, Vancouver, Canada; 10-14 Jul 1989. ©1989, IEEE.)

ed for every observation point along the reference pass. Usually an average of no more than 20 of a possible 22 is available, owing to data dropout from the satellite.¹⁰

Comparison of Absolute Topography with Model Results and *In Situ* Observations

For the Geosat ground track in Figure 2, Figure 3 shows the altimetric mean sea surface consisting of the geoid, the mean ocean signal, and some undetermined orbit error associated with the reference pass. The figure also shows the mean model sea-surface height that is subtracted from the altimetric mean sea surface to obtain an estimate of the synthetic geoid, which is also shown. Figure 4 shows a comparison between the absolute topography computed from the altimeter using the synthetic geoid for 8 October 1987 and the model output along the identical ground track for the same day. The amplitude of the stream as measured by the altimeter is larger than that for the model; however, the placement of the model stream axis and that of the warm-core eddy are within 20 km of each other. The root-mean-square difference between the two height measurements is 22 cm, and the correlation coefficient between the two curves is 0.91. The sources of this difference probably lie in the initialization error of the forecast model, that is, in the placement of the features and in the error caused by the relatively small sample size (20 passes) used to compute the mean altimetric sea surface. Preliminary results are encouraging, but many more passes and comparisons need to be made.

The model results used in the comparison of Figure 4 were also used in the formation of the mean sea surface. Similar comparisons between model results and absolute topography can be made outside the time period of the data used to form the mean. As long as the new data are referenced to the same reference pass, the synthetic geoid method can be used.

An AXBT survey was conducted along this same ground track on 6 May 1987 by the Naval Oceanographic Office. The ocean temperature was measured as a function of depth by dropping AXBT's at a nominal spacing of 20 km along the Geosat ground track. The sea-surface topography was estimated from the temperature-depth profiles after the method of deWitt.¹¹ These observations were made before the time period used to form the mean sea surfaces just discussed. Since the AXBT's measure only the baroclinic (depth-varying) portion of the absolute sea-surface height, the values have an unknown bias associated with the barotropic (depth-independent) component. The blue curve in Figure 5 is the sea-surface height determined from the AXBT's and the black curve is the sea-surface height determined from the Geosat altimeter. Because of an unknown bias, the two curves were made to agree at the point indicated by an asterisk. Figure 5 also shows a deep cold-core eddy at about 37.5°N with a surface depression of about 90 cm and the Gulf Stream at 40°N with an offshore elevation of about 90 cm. The elevation of the stream as measured between the two extremes of height agrees to within 1 cm. Note that the along-track placement of the eddy and the Gulf Stream is coincident. The correlation

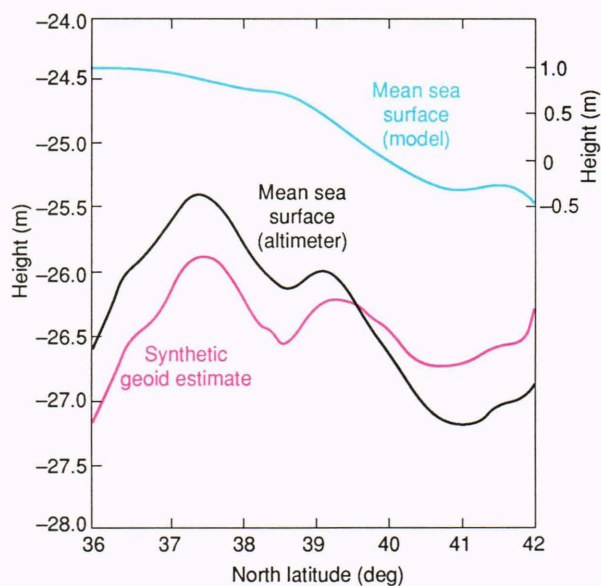


Figure 3. The sea-surface height from the Harvard model (blue curve) for the mean Gulf Stream for the ascending Geosat track shown in Figure 2. The Gulf Stream axis has been arbitrarily set to zero elevation. The black curve is the mean sea surface computed from one year of Geosat altimeter data. The red curve is the synthetic geoid computed by subtracting the mean sea surface of the Harvard model from the altimeter-derived mean sea surface. (Height scale on the right refers to the model mean sea surface.)

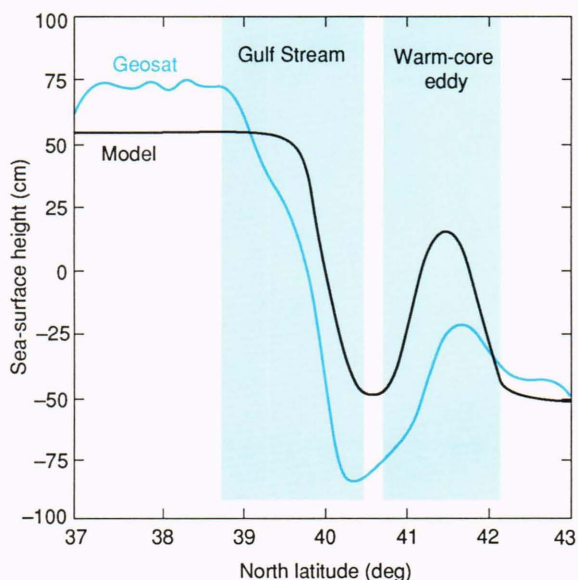


Figure 4. Absolute sea-surface topography computed using the altimetric data for 8 October 1987 and the synthetic geoid (blue curve). The black curve is the corresponding realization of the sea-surface height based on the Gulfcast for that day. A warm-core eddy is located at 41.5°N, and the main core of the Gulf Stream is located at 39.8°N. (Adapted, with permission, from Porter, D. L., Glenn, S., and Robinson, A. R., "Geoid Estimates in the Gulf Stream from GEOSAT Altimetry Data and a Gulfcast Mean Sea Surface," in *IGARSS '89, 12th Canadian Symposium on Remote Sensing, Quantitative Remote Sensing: An Economic Tool for the Nineties*, Vol. 2, Vancouver, Canada; 10-14 Jul 1989. ©1989, IEEE.)

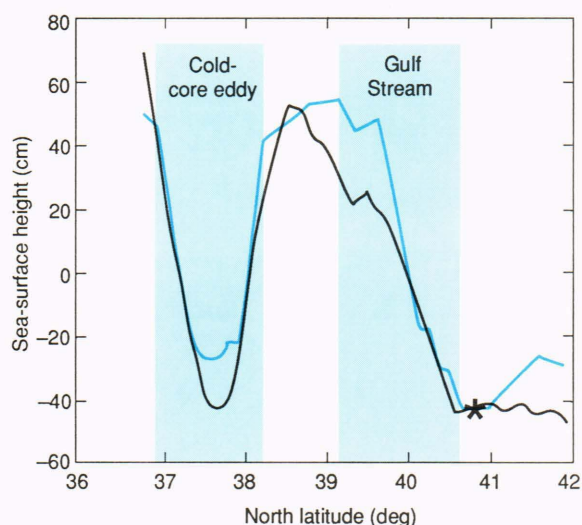


Figure 5. Sea-surface height derived from the temperature at 300 m based on AXBT measurements (blue curve). Absolute topography computed from the Geosat altimeter for 6 May 1987 (black curve). The asterisk indicates the point at which the sea-surface heights of the two curves were set equal to each other. (Adapted, with permission, from Porter, D. L., Glenn, S., and Robinson, A. R., "Geoid Estimates in the Gulf Stream from GEOSAT Altimetry Data and a Gulfcast Mean Sea Surface," in *IGARSS '89, 12th Canadian Symposium on Remote Sensing, Quantitative Remote Sensing: An Economic Tool for the Nineties*, Vol. 2, Vancouver, Canada; 10-14 Jul 1989. © 1989, IEEE.)

coefficient between the sea-surface height derived from the AXBT's and the altimeter is 0.96, and the root-mean-square difference between the two curves is 8.8 cm.

Comparison of the Three Methods

We now give examples of the different methods for analyzing altimetric data for the Geosat ground track in Figure 2. Real-time forecasts for the three days analyzed (31 December 1987 and 3 and 20 February 1988) were based on AXBT and satellite infrared data; no altimetric information was used in that forecast. For each day we computed the sea-surface height from the Harvard model (Fig. 6A); the absolute sea-surface height from the altimeter using the synthetic geoid (Fig. 6B); the altimetric sea-surface-height anomaly about the altimetric mean (Fig. 6C); the sea-surface-height difference from the Harvard model's collinear pass-minus-pass pairs (Fig. 6D); and the sea-surface-height difference from the altimetric collinear pass-minus-pass pairs (Fig. 6E).

The bottom curve in Figure 6A for 31 December 1987 of the Gulfcast has the Gulf Stream at 39.4°N, an edge of a warm-core eddy near 41.5°N, and no cold-core eddies. Figure 6B shows the absolute topography as computed using the synthetic geoid for the same pass. The placement of the Gulf Stream based on the synthetic geoid is farther north than it is for the model, and the warm-core eddy in the model results is also suggested in the absolute topography. But at 37.5°N in Figure 6B a cold-core eddy appears that has a depression of about 50 cm, which is not in the real-time forecast. (Recall that the forecast was based on AXBT and infrared surface

temperature data only and that cold-core eddies south-east of the Gulf Stream lose their infrared sea-surface-temperature signal quickly.)

The bottom curve in Figure 6C, for the same date, is the altimeter sea-surface anomaly (relative to a mean sea surface), which shows two depressions, one near 37.5°N and the other near 40°N. With no *a priori* information, it would be difficult to decide whether the Gulf Stream was near 37.5°N and a warm-core eddy was near 40°N or the Gulf Stream was near 40°N and a cold-core eddy was near 37.5°N. Fortunately, one often has ancillary data from sources such as AXBT's, satellite infrared imagery, or forecasts to remove such ambiguities. Once the ambiguity is resolved, the method of using departures from the mean allows estimates of the position of the Gulf Stream and the eddy. An estimate of the strength of the eddy can also be made. The signal representing the Gulf Stream is greatly reduced, however, since the Gulf Stream estimate is the deviation from the altimetric mean.

For 3 February 1988, Figure 6A shows the Gulf Stream located at approximately 39.5°N, with no evidence of either a cold- or warm-core eddy. The absolute topography shown in Figure 6B for that date shows the Gulf Stream to be broader and weaker than in the model, possibly because the ground track cuts the Gulf Stream obliquely rather than at right angles. Figure 6B also shows evidence of a cold-core eddy near 37.5°N. For the same date, Figure 6C shows that the sea-surface-height anomaly has no clear signal, implying that the individual pass sea-surface-height signal is nearly identical to the mean. There is some suggestion of the cold-core eddy near 37.5°N, but no signal can clearly be designated as the Gulf Stream.

For 20 February 1988, Figure 6A shows the Gulf Stream farther north at 40.2°N. The placement of the Gulf Stream from the model (Fig. 6A), from the absolute sea-surface topography (Fig. 6B), and from the sea-surface-height anomaly (Fig. 6C), all agree to within 0.1° of latitude along the altimeter track.

Let us examine the collinear pass-minus-pass differences. If two passes over the Gulf Stream have identical Gulf Stream signals, but are translated along track, then the difference of those two curves will be either a "U" or an inverted "U"-shaped difference signal. Porter et al.⁴ have shown that the two inflection points of the U-shaped curve correspond to the positions of the Gulf Stream for the two specified days.

For the collinear pass-minus-pass differences, we begin by using the individual pass model sea-surface heights in Figure 6A to interpret the model pass-minus-pass differences in Figure 6D. In Figure 6A, the Gulf Stream is located near 39.4°N on 31 December 1987, 39.5°N on 3 February 1988, and 40.2°N on 20 February 1988. When the model estimate for 3 February is subtracted from the estimate for 20 February (top curve in Fig. 6D), we are left with an inverted U shape in the center, with signal cancellation on either side. The south side of the inverted U gives the Gulf Stream location for 3 February, and the north side gives its location on 20 February. Because the location differs in the two passes, the signal cancel-

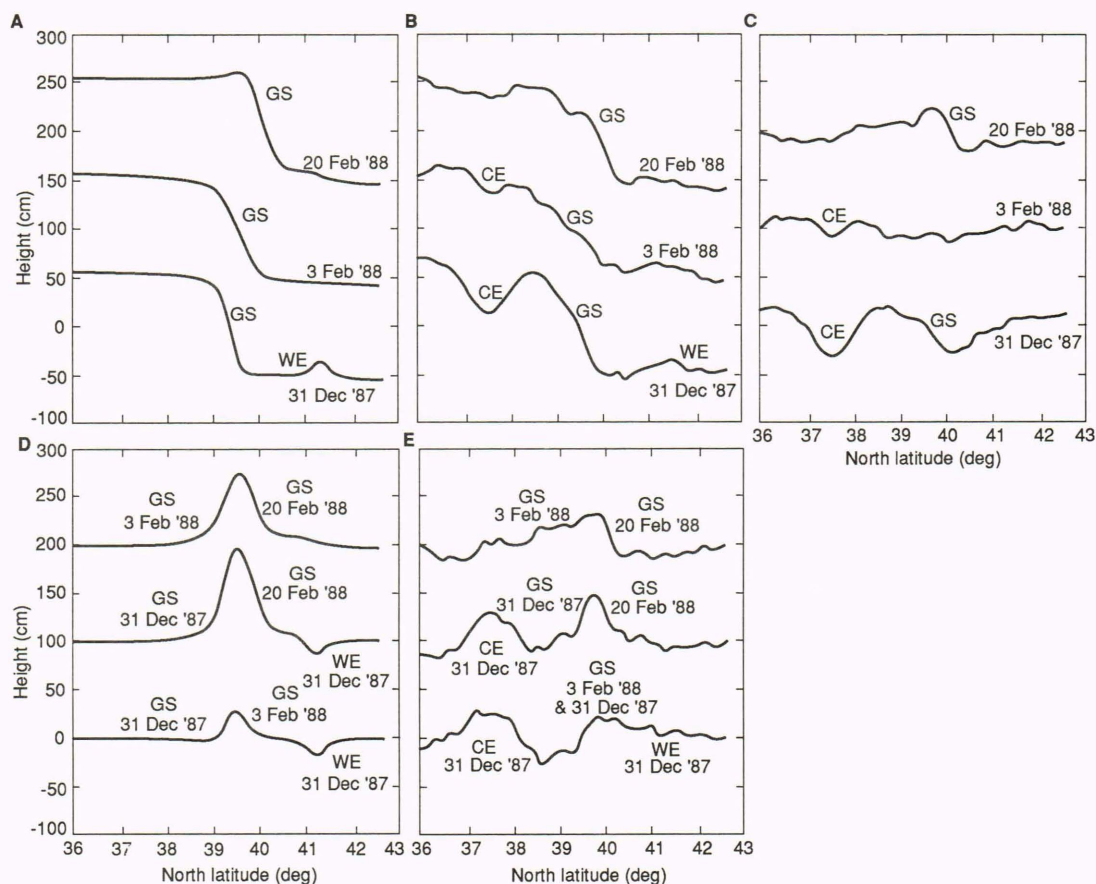


Figure 6. A. Sea-surface heights derived from the Harvard University Gulfcast model. The dates next to the pass correspond to the day the satellite passed over the Geosat track shown in Figure 2. The curves of 3 and 20 February 1988 are offset from the origin by 100 and 200 cm, respectively. B. Sea-surface heights as measured by the altimeter (single pass) minus a synthetic geoid. (Pass and dates as in Fig. 6A.) C. Sea-surface heights measured by the altimeter (single pass) minus a 1-year altimeter mean. (Pass and dates as in Fig. 6A.) D. Sea-surface-height differences between two collinear Harvard model-derived passes. The three curves are the differences for 3 February 1988 minus 31 December 1987 (bottom), 20 February 1988 minus 31 December 1987 (center), and 20 February 1988 minus 3 February 1988 (top). E. Sea-surface-height differences between two collinear altimeter passes. The three curves are the differences for 3 February 1988 minus 31 December 1987 (bottom), 20 February 1988 minus 31 December 1987 (center), and 20 February 1988 minus 3 February 1988 (top). (GS = Gulf Stream, WE = warm-core eddy, CE = cold-core eddy.)

lation is incomplete. When the model estimate from 31 December is subtracted from 20 February (middle curve in Fig. 6D), an inverted U is obtained again for the Gulf Stream difference signal because the two Gulf Stream locations are widely separated, and are thus far enough apart that the full 1-m signal amplitude is preserved. Also in this difference signal, the warm eddy from 31 December appears as a depression below zero. If the warm eddy were in the 20 February signal, it would have appeared as an elevation above zero. (The opposite holds true for cold eddies.) The final pass-minus-pass difference is 3 February minus 31 December (bottom curve in Fig. 6D). Here the Gulf Stream is almost in the same location, so the signal cancellation is nearly complete.

Figure 6E shows the same pass-minus-pass differences calculated from the altimeter data. The inverted U in the 20 February minus 3 February difference (top curve) has a steep northern face and a broad southern face. The altimeter difference indicates that the Gulf Stream

on 20 February is in the expected location, but that the Gulf Stream crossing on 3 February is broader than in the model estimate. In the 20 February minus 31 December difference (middle curve), the inverted U near 40°N clearly indicates the location of the Gulf Stream on both days. As before, the Gulf Stream on 20 February is in the expected location, but on 31 December it is slightly north of the model estimate. Since the two Gulf Stream locations are closer in the altimeter data, the amplitude of the U in the difference signal is less than in the model estimate. Also, the cold eddy present in the 31 December signal appears near 37.5°N as an elevation above zero in the difference signal. The signal cancellation in the last altimeter difference signal, 3 February minus 31 December (bottom curve) indicates that the location of the Gulf Stream in these two passes is nearly identical. Deviations from complete cancellation are caused by the difference between the broad stream crossing on 3 February and the narrow stream crossing on

31 December. Again, the cold-eddy signal is present near 37.5°N.

Real-Time Measurements of the Gulf Stream

Altimeter measurements from Geosat are provided by APL's real-time data system for Geosat. The system computes dynamic topography within 48 hours of the time the measurements are made by the satellite. Computations begin as soon as the sensor data record tapes have been prepared by the Geosat ground station from the satellite telemetry. As described by Calman and Manzi elsewhere in this issue, standard corrections are made for atmospheric and ionospheric propagation and for tides. Once the dynamic topography has been computed using the synthetic geoid, data are transmitted electronically to the Harvard group for use in initializing an ocean forecast model and in optimizing the placement of *in situ* measurements by ship and aircraft.

Two examples of the real-time dynamic topography are shown in Figure 7. Figure 7A contains data for 18 April 1989; the ground track is the green line shown on the model forecast of Figure 1C. Excellent agreement exists between the altimeter and model, both for the elevation (1 m) and the location (37.8°N) of the Gulf Stream; neither data set shows warm or cold eddies. A more complicated example occurred on 12 March 1989 as represented in Figure 7B, whose ground track is the yellow line in Figure 1C. The model forecast for that day was initialized on the basis of satellite infrared imagery alone. Cold eddies with significant subsurface structure that can be detected in the altimetry often are not visible in the infrared imagery, because sea-surface-temperature contrast is lacking. Although the location of the Gulf Stream in the altimeter signal agrees well with the Harvard model estimate, the altimeter clearly shows a cold eddy, near a latitude of 36°N, that was not observed in the imagery and therefore not included in the model initialization. When this occurs, the next model initialization is updated to include the cold eddy in the proper position.

Other Regions and Signal Strength

The Gulf Stream system is one of, if not the most, energetic regions in the world's oceans, and therefore presents a strong surface height that is readily measured by the Geosat altimeter. Many other strategically important regions of the oceans have surface signatures that are only a small fraction of the Gulf Stream's, however. One is the frontal system that lies roughly parallel to the ridge between Iceland and the Faeroe Islands, also called the Greenland, Iceland, United Kingdom (GIUK) Gap. The demonstrated need to acquire extensive knowledge of frontal movement and dynamics in this region has prompted an investigation to determine how effective the Geosat altimeter can be in measuring fronts and eddies in this region, and how this information can be used for nowcasts and in the initialization of dynamic forecast models in the area.¹²

From April to September 1987, AXBT surveys were conducted in the rectangular region between 6° and 11°W and 63° and 66°N to construct and evaluate the Harvard forecast model. The resulting data set afforded the opportunity to explore the concept of extracting a synthetic geoid in the region. To that end, 29 AXBT surveys were objectively analyzed and used to create a mean sea-surface-height map. A contour map of this mean field is shown in Figure 8A with the Geosat altimeter ground tracks used in the study overlaid. To compute a synthetic geoid, a mean height was determined for the Geosat data from the first thirty 17-day cycles (starting 12 November 1986) using the procedures discussed earlier. Because of occasional dropouts, not all means had 30 passes to average, but at least 22 Geosat passes went into a mean for a given ground track. The mean altimetric sea-surface height is shown in Figure 8B along the ground track shown in Figure 8C.

The determination of barotropic modes in the region caused concern because of the small sea-surface heights, which are in general between 20 and 30 cm. A previous study (A. R. Robinson and E. Dobson, unpublished

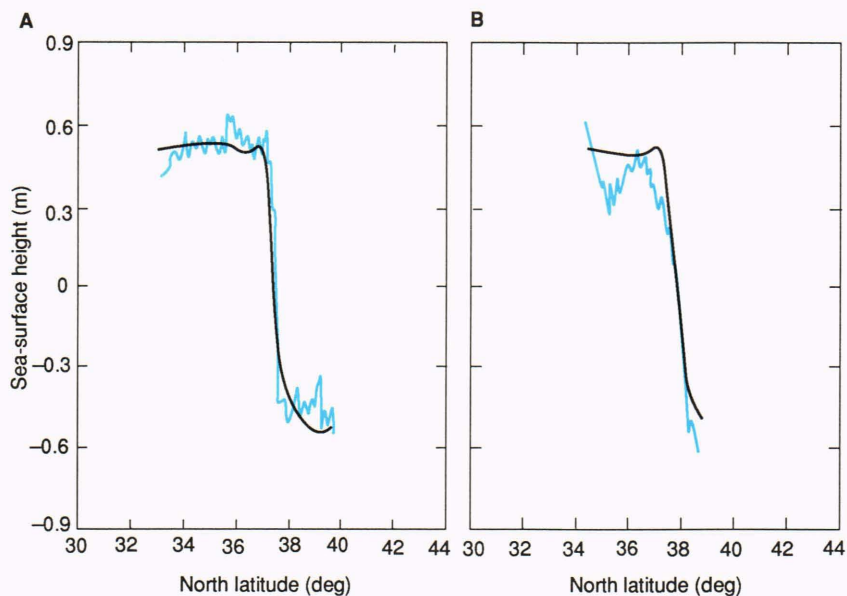


Figure 7. Comparison between the absolute sea-surface height computed from the altimeter (blue curve) and the sea-surface height derived from the model (black curve) for (A) 18 April 1989 and (B) 12 March 1989.

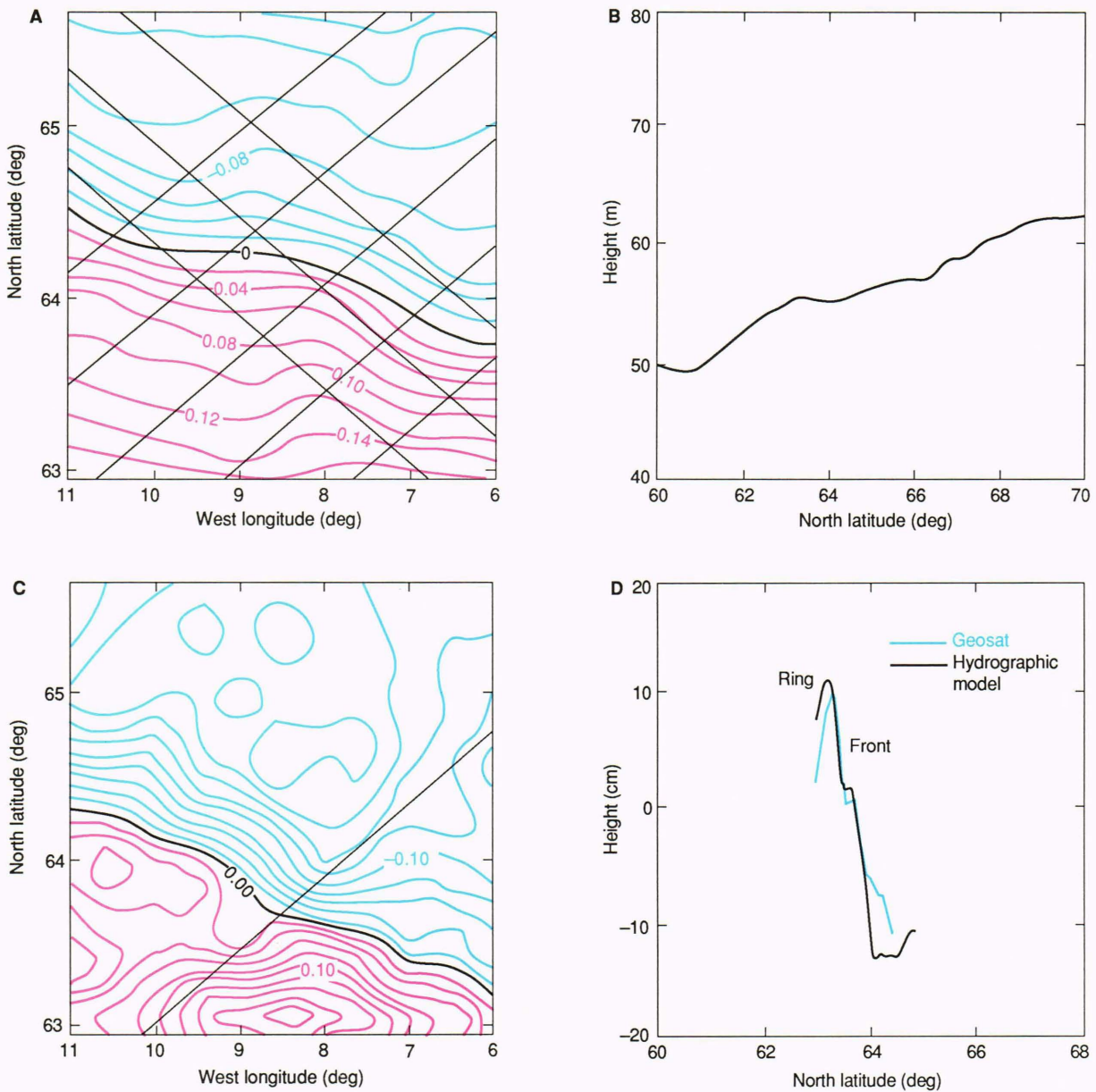


Figure 8. A. Mean sea-surface-height contour map showing Geosat ground tracks (contour interval = 0.02 m). B. Mean altimeter height for the pass shown in panel (C). C. Sea-surface-height contour map for 25 April 1987, with ground track overlaid. D. Geosat altimeter dynamic topography (blue curve) and model dynamic topography (black curve). (Refer to Fig. 1 caption for color code used in A and C.)

data), using pass-minus-pass differences, extensively analyzed and determined the “best” consistent set of daily barotropic modes, and those modes were applied in the analyses. Tidal corrections were also applied to the data. It was determined that as long as ground tracks were not in the region of shelf waters, the Schwiderski tidal model was accurate.¹³

The mean sea-surface height from the model was then subtracted from the Geosat mean to obtain a first estimate of a synthetic geoid in the GIUK Gap. To validate and determine the accuracy of the Geosat topography, we are comparing absolute dynamic topography along given ground tracks for individual days with model

heights along the same ground track. We give one good comparison to show the potential with the synthetic geoid method for obtaining dynamic topography from Geosat height measurements. A contour map of the modeled sea-surface height for 25 April 1987 is shown in Figure 8C, with the Geosat ground track for that day superimposed. The frontal axis is evident from roughly 64.5°N diagonally to 63.5°N, and a large eddy is apparent to the south, with an eddy of lesser strength to the north. The Geosat ground track crosses the front and intersects the western edge of the southern eddy. Figure 8D gives the comparison between the model and the Geosat altimeter, and both measurements show the same

frontal elevation of about 22 cm and the tip of the southern eddy. This work is promising, and a more extensive analysis will be published in the future.

A final example from the northern northeast Atlantic concerns the western front edge of an eddy observed in the summer of 1988 during the Athena Experiment, conducted at sea by French naval oceanographers¹⁴ in collaboration with Harvard scientists, using altimeter data supplied by the APL real-time data system. The high-quality *in situ* database consists of information gathered from hydrographic stations for measuring temperature and salinity versus depth and expendable bathythermographs to determine the baroclinic fields, and a SOund Fixing and Ranging or SOFAR float (sub-surface Lagrangian drifter) to determine the barotropic mode. The model output and comparison shown in Figure 9 were made in real time at sea. The Harvard model system is flexible and portable and has been run on various ships and remote locations in real time since 1986 on MicroVAX, HP, and SUN computers. The inset in Figure 9 shows the model sea-surface-height field in a 210 × 210 km region centered at 25.1°W and 52.6°N. The large-scale mean flow is weak, but the occasional eddies are relatively strong. Methods 1 and 2 (pass-minus-synthetic geoid and pass-minus-mean sea surface, respectively) are identical here, since no contribution from sub-basin-scale mean oceanography is expected. The comparison between the combined *in situ* data and model estimate (e.g., hydrography, float, model) and the altimeter estimate of the absolute topography is excellent for both shape and amplitude (40 cm), as Figure 9 shows.

CONCLUSIONS

A synthetic geoid is an estimate of the medium-spatial-scale components of the true geoid, obtained by removing long-wavelength oceanographic signals, orbit errors, environmental corrections, and a mean mesoscale oceanographic sea surface from a mean sea surface computed using altimetric data. The technique of using the synthetic geoid allows estimates of the absolute sea-surface topography associated with the oceanic mesoscale. To obtain the synthetic geoid, we need a good estimate of the mean sea-surface field over the same time period when the altimetric mean field was formed. The estimated mean field can be derived from models and data. If the mean kinetic energy (MKE) for the area under investigation does not contain sub-basin-scale features, then the estimate of zero for the background mean sea-surface height suffices.

The three different oceanographic areas discussed in this article—the Gulf Stream, the GIUK Gap and the Athena area—have their own distinctive oceanographic signals. The Gulf Stream region has MKE and eddy kinetic energy (EKE) with equal magnitude, and meandering yields a mean feature about 200 km wide. Thus, the removal of the mean Gulf Stream is important in deriving the synthetic geoid. The MKE and EKE resulting from frontal meandering in the GIUK Gap region also are the same order of magnitude, but altimeter sea-surface-

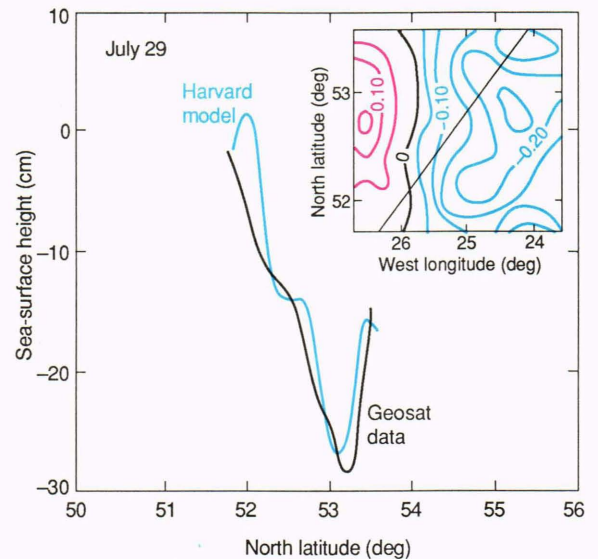


Figure 9. Comparison between sea-surface height determined from the altimeter minus a mean sea surface and the sea-surface height derived from the model. Inset shows the ground track of the altimeter over the nowcast of the Athena area. Blue contours represent negative values; red indicates positive values.

height signals across the front are much smaller than those in the Gulf Stream. It becomes more difficult, but still possible, to obtain absolute sea-surface topography in the GIUK Gap by the same methods used in the Gulf Stream region. In the Athena area, the MKE density is small and the EKE density associated with an occasional eddy feature is much larger; the estimate of the altimetrically-derived mean sea surface is a good estimate of the synthetic geoid.

For a few Geosat passes over the Gulf Stream, we have demonstrated that the absolute sea-surface topography computed using the synthetic geoid agrees well with model results and with *in situ* data. We are now performing thorough quantitative studies comparing the altimeter result with both models and *in situ* data. The synthetic geoid approach for the GIUK Gap shows promise; some initial estimates of the absolute sea-surface topography agree well with model results. A preliminary study in the region of the Athena Experiment, which has little mean oceanography, shows that the use of the mean sea surface as the synthetic geoid gives excellent results. The synthetic geoid is a powerful tool for direct sea-surface-height signal estimates, which are more easily interpreted for research, nowcast, and forecast purposes than the results from the pass-minus-pass and pass-minus-mean methods.

REFERENCES

- Cheney, R., Douglas, B., Agreen, R., Miller, L., Porter, D., et al., *Geosat Altimeter Geophysical Data Record User Handbook*, NOAA Technical Memorandum NOS NGS-46, U.S. Department of Commerce, Rockville, Md. (Jul 1987).
- Robinson, A. R., and Walstad, L. J., "The Harvard Open Ocean Model: Calibration and Application to Dynamical Process, Forecasting, and Data Assimilation Studies," *Appl. Numerical Math.* 3, 89-131 (1987).

³Robinson, A. R., and Walstad, L. J., "Altimetric Data Assimilation for Ocean Dynamics and Forecasting," *Johns Hopkins APL Tech. Dig.* **8**, 267-271 (1987).

⁴Porter, D. L., Walstad, L. J., and Horton, C., *Determination of Mesoscale Features Using Geosat Altimetric Measurements and Verified with Model and In Situ Measurements*, JHU/APL SIR89U-005 (Jan 1989).

⁵Milbert, D., Douglas, B., Cheney, R., and Miller, L., "Calculation of Sea Level Time Series from Non-Collinear Geosat Altimeter Data," *Mar. Geodesy* (in press) (1989).

⁶Glenn, S., Robinson, A., and Spall, M., "Recent Results from the Harvard Gulf Stream Forecasting Program," *Oceanographic Monthly Summary* **7**, 3-13 (Apr 1987).

⁷Walstad, L. J., "Modeling and Forecasting Deep Ocean and Near Surface Mesoscale Eddies," in *Harvard Open Ocean Model Reports*, p. 266 (23 May 1987).

⁸Robinson, A. R., Spall, M. A., and Pinardi, N., "Gulf Stream Simulations and the Dynamics of Ring and Meander Process," *J. Phys. Oceanogr.* **18**, 1811-1853 (1988).

⁹Robinson, A. R., Spall, M. A., Walstad, L. J., and Leslie, W. G., "Data Assimilation and Dynamical Interpolation in GULFCASTING Experiment," in *Dynamics of Atmospheres and Oceans* (in press) (1989).

¹⁰Cheney, R., Douglas, B., Agreen, R., Miller, L., and Doyle, N., *The NOAA Geosat Geophysical Data Records: Summary of the First Year of the Exact Repeat Mission*, NOAA Technical Memorandum NOS NGS-48, U.S. Department of Commerce, Rockville, Md. (Sep 1988).

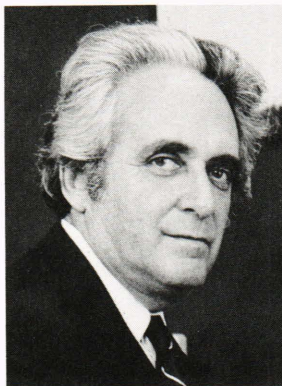
¹¹deWitt, P. W., *Subsurface Temperature Structure as Inferred from Sea-Surface Topography—A Possible Application of Satellite Altimetry*, TR-295, Naval Oceanographic Office (Oct 1986).

¹²Robinson, A. R., Walstad, L. J., Calman, J., Dobson, E. B., Denbo, D. W., et al., "Frontal Signals East of Iceland from the Geosat Altimeter," *Geophys. Res. Lett.* **16**, 77-80 (1989).

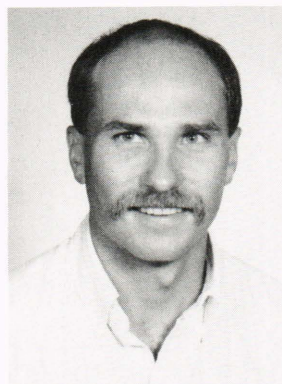
¹³Schwiderski, E. W., "On Charting Global Tides," *Rev. Geophys. Space Phys.* **18**, 243-268 (1980).

¹⁴Le Squire, B., *Rapport sur le traitement des Données de la Campagne Athena 88*, Centre National de Recherches Météorologiques, Toulouse (Jun 1989).

ALLAN R. ROBINSON is the Gordon McKay Professor of Geophysical Fluid Dynamics at Harvard University, where he received B.A. (1954), M.A. (1956), and Ph.D. (1959) degrees in physics. He has served as Director of the Center for Earth and Planetary Physics and Chairman of the Committee on Oceanography. Professor Robinson's research and contributions have encompassed dynamics of rotating and stratified fluids, boundary layers, thermocline dynamics, and the dynamics and modeling of ocean currents and circulation. His research group is currently conducting research in ocean forecasting.



SCOTT M. GLENN received his Sc.D. in 1983 in ocean engineering from the Massachusetts Institute of Technology and Woods Hole Oceanographic Institution Joint Program. He worked as a research engineer in the Offshore Engineering Section of Shell Development Company from 1983 to 1986. He joined Harvard University in 1986 as a project scientist in the Department of Earth and Planetary Sciences, where he is the lead scientist for the Gulf Stream Forecasting Project.



ACKNOWLEDGMENTS—We are grateful to Jack Calman for providing the data for the real-time section and to Leonard J. Walstad and Donald W. Denbo for making available the comparison example for the Athena region. We thank Julius Goldhirsh and Charles Kilgus for interesting discussions during the work. Thanks are also given to Karen Melvin for help in preparing this manuscript, to Eileen Schomp for her assistance in the calculations made for the GIUK Gap region, and to Geraldine Gardner for her help with the real-time Gulf Stream data. This work was supported in part by the Office of Naval Technology through NORDA Contract No. N00014-88-K-6008 to Harvard University, by the Oceanographer of the Navy through NORDA Contract No. N00014-86-K-6002 (also to Harvard University), and by the National Oceanic and Atmospheric Administration and the Geosat Validation Program, both under contract No. N00039-89-C-5301 to JHU/APL.

THE AUTHORS



DAVID L. PORTER received a B.S. in physics from The University of Maryland in 1973, an M.S. in physical oceanography from the Massachusetts Institute of Technology in 1977, and a Ph.D. in geophysical fluid dynamics from the Catholic University of America in 1986. He worked for the National Oceanic and Atmospheric Administration from 1977 through 1987 and was appointed to the senior staff of APL in 1987. He works in the Space Geophysics Group using Geosat data in the analysis of ocean mesoscale variability and winds and waves.



ELLA B. DOBSON has been at APL since 1962 and is a member of the Principal Professional Staff. She received a B.S. degree in mathematics from Fisk University in Nashville in 1960 and a masters degree in numerical science from The Johns Hopkins University in 1970. She is a member of Phi Beta Kappa and Beta Kappa Chi. Ms. Dobson has conducted research on remote sensing of the atmosphere and oceans for most of her career. For the last six years, her research has focused on oceanographic circulation along with winds and waves.